ACCELERATED PUBLICATION

This paper is available online at www.jbc.org

THE JOURNAL OF BIOLOGICAL CHEMISTRY VOL. 282, NO. 34, pp. 24490–24494, August 24, 2007

Structural Basis for the Function of DCN-1 in Protein Neddylation*[S]

Received for publication, March 6, 2007, and in revised form, June 11, 2007
Published, JBC Papers in Press, June 26, 2007, DOI 10.1074/jbc.C700038200

Xiaoyu Yang[‡1], Jie Zhou[‡1], Lei Sun[‡], Zhiyi Wei[‡], Jianying Gao[‡], Weimin Gong[‡], Rui-Ming Xu[§], Zihe Rao[‡¶], and Yingfang Liu[‡2]

From the [‡]National Laboratory of Biomacromolecules, Institute of Biophysics, Chinese Academy of Sciences, Beijing 100101, China, the [§]Structural Biology Program, Helen L. and Martin S. Kimmel Center for Biology and Medicine at the Skirball Institute of Biomolecular Medicine and Department of Pharmacology, New York University School of Medicine, New York, New York 10016, and the [¶]Laboratory of Structural Biology, Tsinghua University, Beijing 100084, China

Covalent modification by Nedd8 (neddylation) stimulates the ubiquitin-protein isopeptide ligase (E3) activities of Cullins. DCN-1, an evolutionarily conserved protein, promotes neddylation of Cullins *in vivo*, binds directly to Nedd8, and associates with Cdc53 in the budding yeast *Saccharomyces cerevisiae*. The 1.9 Å resolution structure of yeast DCN-1 shows that the region encompassing residues 66–269 has a rectangular parallelepiped-like all α-helical structures, consisting of an EF-hand motif N-terminal domain and a closely juxtaposed C-terminal domain with six α-helices. The EF-hand motif structure is highly similar to that of the c-Cbl ubiquitin E3 ligase. We also demonstrate that DCN-1 directly binds to Rbx-1, a factor important for protein neddylation. The structural and biochemical results are consistent with the role of DCN-1 as a scaffold protein in a multisubunit neddylation E3 ligase complex.

Ubiquitin-like proteins, such as Nedd8/Rub1, can be covalently attached to substrate proteins in a manner similar to ubiquitination. Modification by Nedd8, a process known as neddylation, has been found in Cullins and several other cellular proteins (1, 2). Neddylation and ubiquitination use parallel mechanisms; each involves their own E1,[3] E2, and E3 proteins, and both follow a sequential modification process. During neddylation, the Nedd8 E1 heterodimer activates Nedd8 in an ATP-dependent process, and the enzyme and Nedd8 form a reaction intermediate through a thioester bond. The activated Nedd8 is then transferred to the conjugating enzyme E2, which also covalently links Nedd8 through a thioester bond. Next, the E2 interacts with an E3 to transfer Nedd8 through an isopeptide bond to a lysine residue of the substrate. The Nedd8 acceptor lysine is located in the C-terminal region of the Cullin family of ubiquitin E3 proteins (2). Cullins and p53 are the only neddylation substrates known to date (1–3).

Protein ubiquitination usually leads to substrate degradation by the proteasome, whereas neddylation of Cullins increases their ubiquitin ligase activities (4–6). At present, Rbx-1 is the only protein known to have a Nedd8 E3 function (7, 8). Rbx-1 contains a single RING motif, and it is an inefficient ubiquitin E3 on its own. This is reminiscent of many E3 ubiquitin ligases; a single RING domain is either incapable of promoting or inefficient to promote ubiquitin transfer. Recently, Kurz *et al.* (9) reported that a novel protein, DCN-1 (defective in Cullin neddylation-1), is important for Cdc53 (Cullin-1) neddylation in the budding yeast. DCN-1 is a conserved protein found in organisms ranging from fungi to mammals. Interestingly, a human DCN-1 homolog protein (see HUMA1 in Fig. 1*A*), also known as SCCRO (squamous cell carcinomas-related oncogene), is an oncogene (10) and possibly functions in the hedgehog signaling pathway by activating Gli1 expression. DCN-1 contains a predicted N-terminal UBA3 motif and a conserved C-terminal DUF298 domain of unknown function. Studies from yeast and *Caenorhabditis elegans* showed that DCN-1 directly binds Nedd8 (yeast ortholog is Rub1) and associate with Cdc53. The level of Cdc53 neddylation is greatly reduced in yeast cells lacking DCN-1. Our structural and biochemical analyses reveal that DCN-1 is likely to serve as a scaffold protein mediating protein-protein interactions in a neddylation E3 ligase complex that includes Rbx-1.

EXPERIMENTAL PROCEDURES

Protein Expression and Crystallization—Recombinant full-length yeast DCN-1 was expressed in *Escherichia coli* as a GST fusion protein using a pGEX-4T-2 vector (Amersham Biosciences). GST-DCN-1 was first purified on a GSH-agarose affinity column followed by the removal of the GST tag with thrombin digestion. Briefly, cell lysate in 1× PBS (pH 7.4) buffer was centrifuged with 20,000 × *g* for 1 h, and the supernatant was loaded onto GST affinity column. After intensive washing with PBS buffer, the GST fusion protein was eluted with GST elution buffer containing 100 mM Tris-HCl(pH 8.0), 50 mM NaCl, and 10 mM reduced glutathione. Further purification of DCN-1 was carried out using successive chromatography steps on ion exchange Q and Superdex-200 columns (Amersham Biosciences) by standard purification methods. Mutations in DCN-1 were introduced by PCR, and mutant proteins were expressed and purified similar to that described for the wild-type protein. GST-fused yeast Rbx-1 (GST-Rbx1) was expressed in *E. coli* and purified using a GSH column.

Crystals were grown by the hanging drop vapor diffusion method at 16 °C. Best diffracting crystals were obtained in a condition containing 100 mM Tris-HCl (pH 8.5), 30% ethylene

* This work was supported by Project '863' grant named as "Structural Study of Cancer-related Proteins." Project '973' (number 2007 CB914304). The costs of publication of this article were defrayed in part by the payment of page charges. This article must therefore be hereby marked "*advertisement*" in accordance with 18 U.S.C. Section 1734 solely to indicate this fact.

The atomic coordinates and structure factors (codes 2IS9) have been deposited in the Protein Data Bank, Research Collaboratory for Structural Bioinformatics, Rutgers University, New Brunswick, NJ (http://www.rcsb.org/).

[S] The on-line version of this article (available at http://www.jbc.org) contains a supplemental method and four supplemental figures.

[1] Both authors contributed equally to this work.

[2] To whom correspondence should be addressed. E-mail: liuy@ibp.ac.cn.

[3] The abbreviations used are: E1, ubiquitin-activating enzyme; E2, ubiquitin carrier protein; E3, ubiquitin-protein isopeptide ligase; GST, glutathione *S*-transferase; PBS, phosphate-buffered saline; SIRAS, single isomorphous replacement with anomalous signal.

TABLE 1
Statistics of crystallographic analysis

Data collection statistics		
Crystal	$K_{2B}PtClB_4$ derivative	Native
Resolution (Å)	1.92	2.42
R_{symB}(%)[a]	3.8 (28.2)[b]	7.8 (51.4)
$\langle I/\sigma \rangle$	54.7 (4.9)	28.3 (7.7)
Redundancy	7.7 (7.4)	6.6 (6.5)
Unique reflections	26193	13179
Completeness[c] (%)	99.9 (99.0)	99.9 (99.4)
Refinement statistics		
Resolution (Å)	64.42–1.92	
Reflections used for refinement	24838	
Reflections used for test set	1328	
Final R/R_{free}[d] (%)	20.3/24.8	
r.m.s.d.[e] bonds/angles (Å)	0.01 Å/1.132°	
Mean *B* value ($Å^2$)	18.7	
Protein/solvent atoms	1739/132	
Ramachandran plot statistics		
Most favorable	95%	
Additionally allowed	4.5%	
Disallowed	0.5% (ASN 85)	

[a] $R_{sym} = \sum I - \langle I \rangle / \sum \langle I \rangle$, where I is the intensity and $\langle I \rangle$ is the averaged intensity of multiple measurements. The summation is over all measured reflections.
[b] Values in parentheses are that of the highest resolution shell.
[c] For the single wavelength anomalous diffraction (SAD) data set, Friedel pairs were counted as independent.
[d] Calculated from 5% of the reflections set aside in refinement.
[e] r.m.s.d., root mean square deviation.

glycol monomethyl ether (PEGMME)-5000, and 0.2 M ammonium sulfate. A platinum derivative was obtained by soaking the crystal in the presence of 0.1 mM K_2PtCl_4. Native and derivative data sets were collected using a home source FR-E SuperBright rotating anode x-ray source equipped with an R-AXIS IV++ imaging plate detector (Rigaku). Data were collected at 100 K and processed using the HKL2000 program suite (11). The crystals belong to the $I4_1$ space group with cell dimensions of $a = b = 81.40$ Å and $c = 106.06$ Å, and there is one molecule per asymmetric unit. Data statistics are shown in Table 1.

Structure Determination and Refinement—The structure of DCN-1 was solved by the method of single isomorphous replacement with anomalous signal (SIRAS) using the platinum derivative data (12). SHELXD (13), XPREP (Bruker) programs were used to locate one platinum atom position, and phasing was carried out using SHARP (14). The SIRAS phase was extended to 1.92 Å and improved with solvent flattening and histogram matching using DM and SOLOMON (15). A model with most of the side chains built by ARP/wARP (16) was refined using CNS (17, 18). Manual adjustment of the model was carried out using the program O (17, 18). The final model contains 205 residues and has an *R*-factor of 20.3% and an R_{free} of 24.8% (see Table 1 for detailed statistics). The atomic coordinates and diffraction data have been deposited in the Protein Data Bank with accession code 2IS9. Structural figures were prepared using PyMOL.

Protein Interaction Assay—Purified GST-Rbx1 was first immobilized on GSH resins followed by the addition of ~10-fold molar excess of purified wild-type DCN-1 or DCN-1 (141–269). Extensive wash of the GSH resins with PBS (pH 7.4) removes unbound proteins, and the bound protein was eluted from the GSH resins with GST elution buffer containing 10 mM reduced glutathione. The eluted sample was then analyzed by Western blotting using an anti-yDCN-1 polyclonal antibody. The antibody was raised in rabbit with purified yeast DCN-1 following a standard protocol, and the quality of the antibodies was monitored by standard Western blots.

RESULTS

We have solved a 1.92 Å crystal structure of yeast DCN-1. The full-length protein has 269 amino acids, and structure revealed an ordered core domain encompassing residues 66–269 (Fig. 1*A*). The disordered N-terminal region contains an ubiquitin-binding UBA3 motif. The refined model has an *R*-factor of 20.3% and an *R*-free of 24.8% and also has high stereochemical quality, with 95% of the residues in the most favored region of the Ramachandran plot, calculated using PROCHECK (19). A section of the SIRAS-phased electron density map and detailed refinement statistics can be found in Fig. 1*B*.

Overall Structure—The all α-helical structure comprises 11 helices in total and can be further divided into two domains: an N-terminal domain (residues 66–158) encompassing helices α1–α5 and a C-terminal domain (residues 159–269) containing helices α6–α11 (Fig. 2*A*). The two domains are in close juxtaposition and rigidly held together with extensive hydrophobic and polar interactions. The rectangular parallelepiped-like structure has approximate dimensions of 64 Å × 27 Å × 24 Å.

Unexpectedly, four of the N-terminal domain helices, α1, α2, α3, and α4, adopt two EF-hand folds. The first EF-hand is composed of α1 and α2, which are connected through a 7-residue loop (loop 1, residues 83–89), whereas helices α3 and α4 form the second EF hand with a 10-residue loop (loop 3, residues 117–126) connecting the two helices (Fig. 2*A*). The N-terminal portion of α5 contacts α1 and α2 at their ends opposite to the connecting loop, and it packs against α3 and α4 in a perpendicular manner. However, the EF-hands have no calcium ion bound in the structure, possibly because: 1) loop 1 is shorter than a canonical EF-hand loop, and it lacks conserved acidic residues; and 2) although loop 3 has a suitable length, it also lacks conserved acidic residues.

The C-terminal domain contains six α-helices (α6–α11), four of which (α6–α9) are arranged in an anti-parallel manner with α6 packs on one side of the α7–α9 plane and α8 on the opposite side. The C-terminal helices α10 and α11 are positioned next to α8 and α9 on the side opposite to helices α6 and α7 and form one end of the elongated structure of DCN-1 (Fig. 2*A*). Interestingly, the distribution of conserved and charged residues on the protein surface differs significantly between two opposite sides of the rectangular parallelepiped-like protein (Fig. 2*B*). The convex side (side 1), which includes α2, α3, and α7, is enriched with negatively charged residues, most of which are not conserved (Fig. 2, *B1* and *B3*). The concave side (side 2) is formed by helices α4, α6, and α9, and this side of the protein surface is enriched with positively charged residues, many of which, such as Lys-180 and Lys-225, are highly conserved (Fig. 2, *B2* and *B4*). The location of conserved residues on the positively charged side of the protein surface suggests an evolutionarily conserved role of this area of the protein surface.

The C-terminal domain is highly conserved among different species, with 9 invariant residues located within the last 29 amino acids, which encompass helices α10 and α11 (Fig. 1*A*). There are 7 acidic residues within the stretch of 29 amino acids in yeast DCN-1, making it highly negatively charged (Fig. 2*B*).

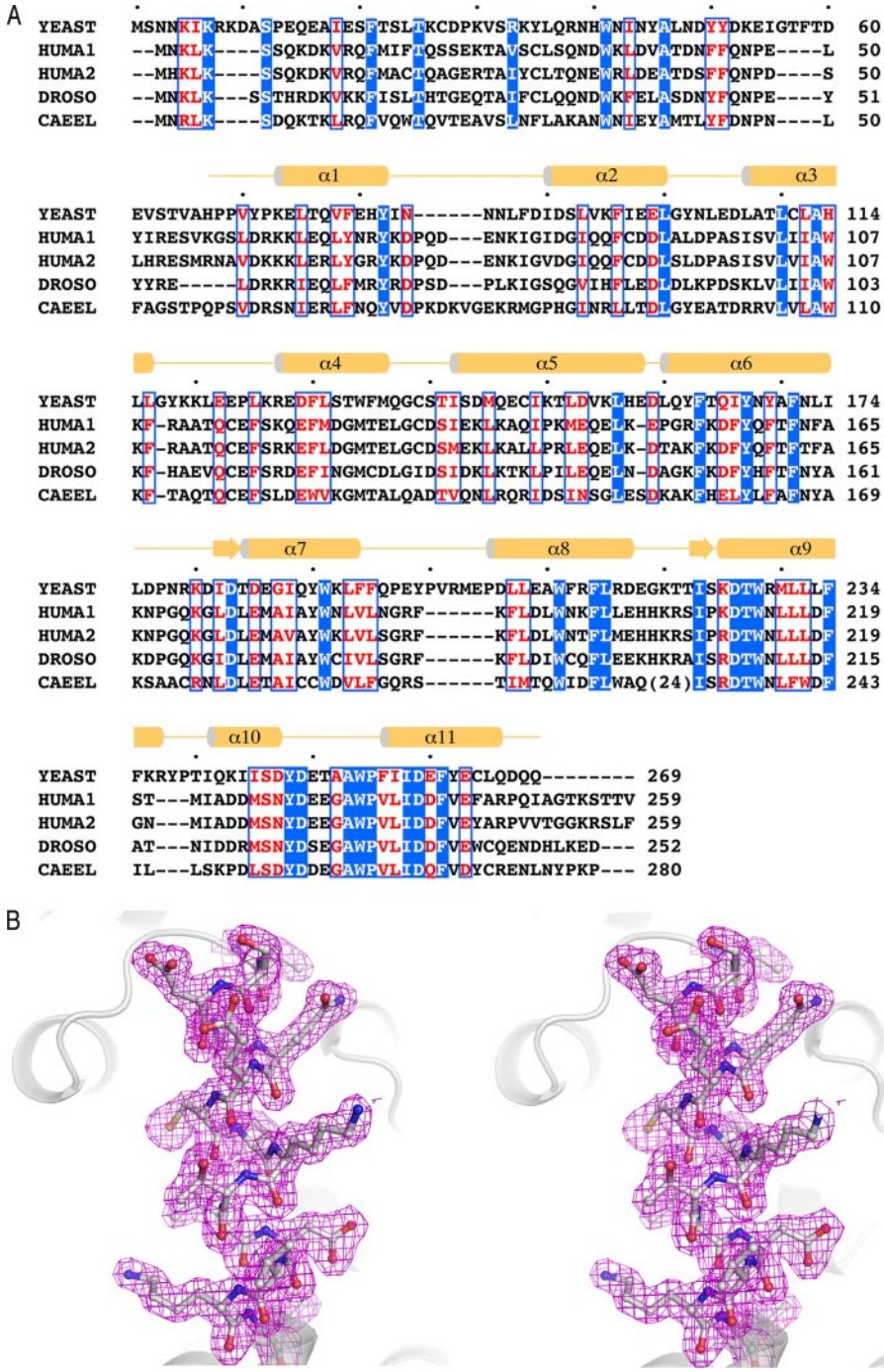

FIGURE 1. *A*, sequence alignment of DCN-1 proteins. Amino acid sequences of yeast, human (HUMA1 and HUMA2), *Drosophila* (DROSO), and *C. elegans* (CAEEL) proteins were aligned using CLUSTALW. Residues identical in all five proteins are shown in *white letters* over a *blue background*; similar residues are shown in *red letters* enclosed in *blue boxes*. Residue numbers and secondary structure elements are shown above the sequences. *B*, a stereo view of a section of the 2.0 Å platinum SIRAS-phased electron density map around helix α5. The map is contoured at the 1.5 σ level. A refined DCN-1 structure is superimposed as a *stick model* (carbon in *gray*; nitrogen in *blue*; and oxygen in *red*).

The high degree of sequence conservation and the unusual surface charge distribution suggest a protein-protein interaction role of the C-terminal domain of DCN-1, although the precise functional significance of this structural feature is currently unknown.

Structural Similarity between DCN-1 and c-Cbl—A search for similar protein structures using the DALI server (20) revealed significant structural homology (with a Z-score of 7.5 using yeast DCN-1 residues 74–159 as the template) between the N-terminal domain of DCN-1 and the EF-hand domain of c-Cbl, which is an ubiquitin E3 ligase that recognizes activated receptor tyrosine kinases (21). The two domains can be superimposed with a root mean squared deviation of 2.7 Å, using the Cα positions of residues located in α1–α4 for alignment (Fig. 3*A*), although the two domains share little sequence identity (<10%). As in DCN-1, the first EF-hand of c-Cbl does not bind a calcium ion. The second EF-hand of c-Cbl binds one calcium ion. However, the interactions deviate from that found in canonical EF-hands. For example, a main chain carbonyl group and the hydroxyl group of a threonine in c-Cbl are also involved in calcium binding.

It is interesting to note that c-Cbl also has a helical module as part of the tyrosine kinase binding (TKB) domain (21). Although it was called a four-helix bundle, the four helices in the TKB domain are arranged in manner better resembling the packing of a pair of parallel coiled-coils that are also characteristic of four of the helices (α6–α9) in the C-terminal domain of DCN-1. However, the four helices in c-Cbl are longer and, unlike the C-terminal domain of DCN-1, they are located N-terminal to the EF-hand domain. The spatial arrangement of the two helical domains with respect to their EF-hand is also different (Fig. 3*B*). Nevertheless, both helical domains of c-Cbl and DCN-1 pack against their respective EF-hand domains through extensive interactions with the second EF-hand. The described structural similarity between DCN-1 and c-Cbl, which is an ubiquitin E3 ligase, suggests a functional parallel between the two proteins, namely, DCN-1 may function as a component of the neddylation E3 ligase.

Direct Interaction between DCN-1 and Rbx-1—To explore the hypothesis that DCN-1 may function in a Nedd8 E3 ligase complex, we tested for direct interactions of yeast DCN-1 with the RING finger protein Rbx-1. Purified GST-Rbx1 was immobilized on GSH resins, and purified untagged DCN-1 was added

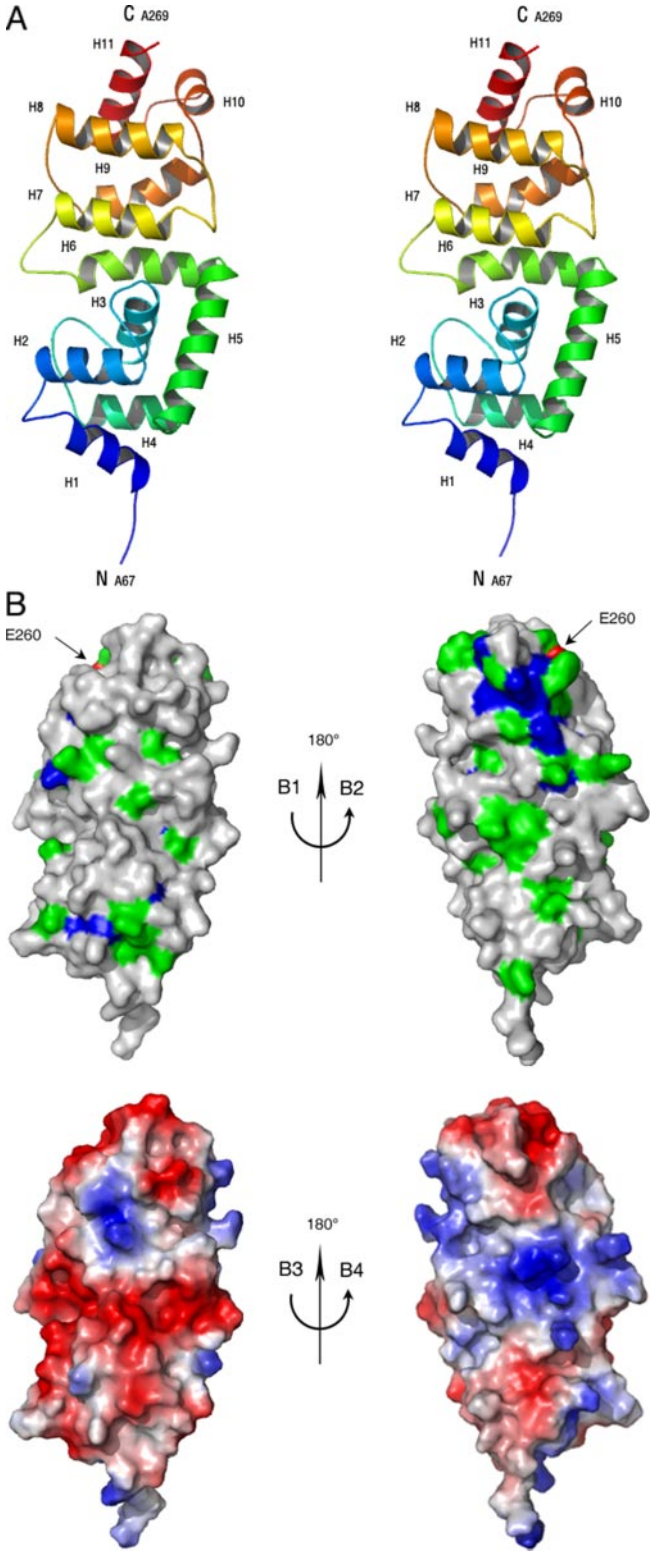

FIGURE 2. **Structure of DCN-1.** *A*, a stereo ribbon diagram showing the overall structure of DCN-1. The structure is colored from the N to the C termini with *blue* to *red*. *B*, a surface representation of the DCN-1 structure. *B1* (*side 1*) and *B3* (*side 2*) show the distribution of conserved residues on the two sides of the protein surface. Absolutely conserved residues are indicated in *blue*, and highly conserved residues are shown in *green*, using the convention defined in the legend for Fig. 1. The *arrow* points to the position of Glu-260, which is colored in *red*. Electrostatic potential on the protein surface is shown in *B2* and *B4*, which are oriented the same as in *B1* and *B3*, respectively. Positively charged regions are shown in *red*, negatively charged regions are in *blue*, and neutral ones are in *white*.

to the GST-Rbx1-bound GSH resins in 10-fold molar excess (Fig. 4*A*). After extensive wash with the binding buffer, proteins bound to the GSH resins were eluted with a buffer containing 10 mM glutathione. Western blotting of the eluted sample using a polyclonal anti-yDCN-1 antibody shows that DCN-1 co-eluted with GST-Rbx1, whereas DCN-1 was not retained on GST-bound GSH resins in a control experiment (Fig. 4*B*). Thus, DCN-1 interacts with Rbx-1 directly *in vitro*. We further measured the binding affinity between DCN-1 and Rbx-1 using the surface plasmon resonance technique (BiAcore) (see Supplemental Data). The results show that DCN-1 binds to GST-Rbx1 with an apparent equilibrium dissociation constant (K_d) of 2.7 μM (see supplemental data). This observation is consistent with and extends a previous observation that DCN-1, Cdc53, and Rbx-1 can coexist in a multiprotein complex (9).

To determine which region of DCN-1 interacts with Rbx-1, several truncation mutants of DCN-1 were engineered, and the DCN-1 variants were expressed in *E. coli* and purified in a manner similar to that for the full-length DCN-1. GST pulldown experiments with purified GST-Rbx1 showed that a C-terminal fragment of DCN-1 encompassing residues 141–269 binds to Rbx-1 with an affinity comparable with that of the wild-type DCN-1 (Fig. 4*B*). Thus, the C-terminal domain of DCN-1 is sufficient for interaction with Rbx-1.

To pinpoint the DCN-1 residues important for interaction with Rbx-1, we made a number of point mutations of highly conserved residues within the C-terminal domain of DCN-1. These mutants include two single point mutations, S1(Q165A) and S2(E260A); four double mutations, D1(K180S/D183S), D2(D249S/D259S), D3(K225A/D226K), and D4(D185R/R216S); and three triple mutations, T1(D247A/D249S/D259S), T2(E263A/D249S/ D259S), and T3(W254G/D249S/D259S). These mutant DCN-1 proteins were used in GST pulldown and Western blotting analyses. Among all of the DCN-1 mutants tested, only S2(E260A) showed a significant loss of binding to Rbx-1 (Fig. 4*C*). Thus, Glu-260 is important for binding Rbx-1, whereas the functions of other conserved residues remain to be elucidated. The structure shows that Glu-260 extends its side chain out from helix α10 and forms a contiguous exposed surface area with three adjacent residues, Glu-250, Phe-256, and Glu-263 (Fig. 2*B*). These residues are also highly conserved (Fig. 1*A*); thus, the surface region occupied by the 4 residues may have an evolutionarily conserved role of interacting with Rbx-1.

DISCUSSION

Our structural study revealed an unexpected resemblance between the structures of DCN-1 and an ubiquitin E3 ligase, c-Cbl. Previous studies have shown that DCN-1 also interacts with Cullin, Nedd8, and ubiquitin (9). We have also demonstrated that DCN-1 interacts directly with Rbx-1p via the C-terminal helical domain in this study. These results together suggest that DCN-1 functions as a component of the Nedd8 E3 ligase complex.

It is clear that DCN-1 cannot function as a Nedd8 E3 ligase on its own. It lacks a RING domain or HECT (homologue to EGAP C terminus) domain associated with all ubiquitin E3 enzymes known to date, and the mechanistic similarity

FIGURE 3. **Superposition of c-Cbl and DCN-1.** *A*, a stereo diagram of superimposed DCN-1 (*blue*) and c-Cbl (*gray*) EF-hand motifs. A *red sphere* represents a calcium ion bound to the c-Cbl EF-hand motif. *B*, superposition of c-Cbl (only EF-hand and helix bundle motifs are shown) with DCN-1 to show the different spatial arrangement of the two helix bundle motifs.

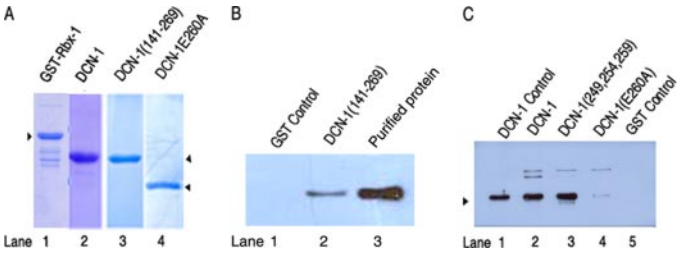

FIGURE 4. **Interaction of DCN-1 and Rbx-1.** *A*, Coomassie Blue-stained SDS-PAGE gels showing purified GST-Rbx1, DCN-1, DCN-1(E260A), and DCN-1 (141–269) proteins (indicated with *triangle pointers*) used for binding experiments. *B*, DCN-1 C-terminal domain (141–269) pulldown with GST-Rbx1 immobilized on GSH resins. *Lane 1*, DCN-1 (141–269) pulldown with GST; *lane 2*, the C-terminal domain (amino acids 141–269) of DCN-1 pulldown by GST-Rbx1; *lane 3*, input of purified DCN-1 (141–269). *C*, Asp-260 of DCN-1 is important for interaction with Rbx-1. *Lane 1*, DCN-1 protein as a positive control; *lanes 2–4*, wild-type DCN-1, a DCN-1 triple mutant (W254G/D249S/D259S), and an E260A mutant of DCN-1 were tested for pulldown by GST-Rbx1; *lane 5*, wild-type DCN-1 pulldown by GST as a negative control. An anti-yeast DCN-1 rabbit polyclonal antibody was used in the Western blots shown in *B* and *C*.

between protein ubiquitination and neddylation implicates the requirement of one of those domains in the Nedd8 E3 enzyme. Previous studies have shown that Rbx-1 could serve as the RING domain protein in the Nedd8 E3 complex. When compared with the prototypical active RING domain ubiquitin E3 ligase c-Cbl, it is possible that the "missing" RING domain of DCN-1 is provided in *trans* by Rbx-1. This is a particularly attractive hypothesis from a structural point of view because c-Cbl contains a RING domain in *cis* with the EF-hand and TKB domains, and the RING domain is positioned next to the helical TKB domain. A similar arrangement of the RING domain of Rbx-1 with respect to the helical domain DCN-1 is likely, as we have shown that the two domains interact directly. Future biochemical and structural studies will determine the precise mode of interaction among DCN-1, Rbx-1, and Cdc53.

Acknowledgments—We are grateful to Yuanyuan Chen for help with BiAcore affinity experiments and Dr. Chonglin Yang, Dr. Fei Sun, Cheng Zhang, and Xueqi Liu for valuable discussions and Yi Han for data collection.

REFERENCES

1. Xirodimas, D. P., Saville, M. K., Bourdon, J. C., Hay, R. T., and Lane, D. P. (2004) *Cell* **118,** 83–97
2. Pan, Z. Q., Kentsis, A., Dias, D. C., Yamoah, K., and Wu, K. (2004) *Oncogene* **23,** 1985–1997
3. Parry, G., and Estelle, M. (2004) *Semin. Cell Dev. Biol.* **15,** 221–229
4. Morimoto, M., Nishida, T., Honda, R., and Yasuda, H. (2000) *Biochem. Biophys. Res. Commun.* **270,** 1093–1096
5. Osaka, F., Saeki, M., Katayama, S., Aida, N., Toh, E. A., Kominami, K., Toda, T., Suzuki, T., Chiba, T., Tanaka, K., and Kato, S. (2000) *EMBO J.* **19,** 3475–3484
6. Read, M. A., Brownell, J. E., Gladysheva, T. B., Hottelet, M., Parent, L. A., Coggins, M. B., Pierce, J. W., Podust, V. N., Luo, R. S., Chau, V., and Palombella, V. J. (2000) *Mol. Cell. Biol.* **20,** 2326–2333
7. Morimoto, M., Nishida, T., Nagayama, Y., and Yasuda, H. (2003) *Biochem. Biophys. Res. Commun.* **301,** 392–398
8. Kamura, T., Conrad, M. N., Yan, Q., Conaway, R. C., and Conaway, J. W. (1999) *Genes Dev.* **13,** 2928–2933
9. Kurz, T., Ozlu, N., Rudolf, F., O'Rourke, S. M., Luke, B., Hofmann, K., Hyman, A. A., Bowerman, B., and Peter, M. (2005) *Nature* **435,** 1257–1261
10. Sarkaria, I., P, O. C., Talbot, S. G., Reddy, P. G., Ngai, I., Maghami, E., Patel, K. N., Lee, B., Yonekawa, Y., Dudas, M., Kaufman, A., Ryan, R., Ghossein, R., Rao, P. H., Stoffel, A., Ramanathan, Y., and Singh, B. (2006) *Cancer Res.* **66,** 9437–9444
11. Otwinowski, Z., and Minor, W. (1997) *Methods Enzymol.* **276,** pp. 307–326
12. Lu, X., Guo, J., and Hsieh, T. C. (2003) *Cell Cycle* **2,** 59–63
13. Sheldrick, G. M. (1998) *Direct Methods for Solving Macromolecular Structures*, pp. 401–411, Kluwer Academic Publishers, Dordrecht, The Netherlands
14. De La Fortelle, E., Bricogne, G. (1997) *Methods Enzymol.* **276,** 472–494
15. Collaborative Computational Project, Number Four (1994) *Acta Crystallogr. Sect. D Biol. Crystallogr.* **50,** 760–763
16. Perrakis, A., Morris, R., and Lamzin, V. S. (1999) *Nat. Struct. Biol.* **6,** 458–463
17. Brunger, A. T., Adams, P. D., Clore, G. M., DeLano, W. L., Gros, P., Grosse-Kunstleve, R. W., Jiang, J. S., Kuszewski, J., Nilges, M., Pannu, N. S., Read, R. J., Rice, L. M., Simonson, T., and Warren, G. L. (1998) *Acta Crystallogr. Sect. D Biol. Crystallogr.* **54,** 905–921
18. Jones, T. A., Zou., J. Y, Cowan, S. W., and Kjeldgaard, M. (1991) *Acta Crystallogr. Sect. A* **47,** 110–119
19. Laskowski, R. A., MacArthur, M. W., Moss, D. S., and Thornton, J. M. (1993) *J. Appl. Crystallogr.* **26,** 283–291
20. Holm, L., and Park, J. (2000) *Bioinformatics* **16,** 566–567
21. Zheng, N., Wang, P., Jeffrey, P. D., and Pavletich, N. P. (2000) *Cell* **102,** 533–539